INTERNATIONAL JOURNAL OF ROBUST AND NONLINEAR CONTROL
Int. J. Robust Nonlinear Control 2016; **26**:1051–1072
Published online 13 May 2015 in Wiley Online Library (wileyonlinelibrary.com). DOI: 10.1002/rnc.3351

Convergence analysis using the edge Laplacian: Robust consensus of nonlinear multi-agent systems via ISS method

Zhiwen Zeng, Xiangke Wang*,† and Zhiqiang Zheng

College of Mechatronic Engineering and Automation, National University of Defense Technology, Changsha, 410073, China

SUMMARY

This study develops an original and innovative matrix representation with respect to the information flow for networked multi-agent system. To begin with, the general concepts of the edge Laplacian of digraph are proposed with its algebraic properties. Benefit from this novel graph-theoretic tool, we can build a bridge between the consensus problem and the edge agreement problem, we also show that the edge Laplacian sheds a new light on solving the leaderless consensus problem. Based on the edge agreement framework, the technical challenges caused by unknown but bounded disturbances and inherently nonlinear dynamics can be well handled. In particular, we design an integrated procedure for a new robust consensus protocol that is based on a blend of algebraic graph theory and the newly developed cyclic-small-gain theorem. Besides, to highlight the intricate relationship between the original graph and cyclic-small-gain theorem, the concept of edge-interconnection graph is introduced for the first time. Finally, simulation results are provided to verify the theoretical analysis. Copyright © 2015 John Wiley & Sons, Ltd.

Received 26 April 2014; Revised 8 January 2015; Accepted 10 April 2015

KEY WORDS: edge Laplacian; edge agreement; leaderless consensus; nonlinear dynamics; small gain

1. INTRODUCTION

Recent decades have witnessed tremendous interest in investigating the distributed coordination of multi-agent systems due to broad applications in several areas including formation flight [1], coordinated robotics [2], sensor fusion [3], and distributed computations [4]. Recently, the consensus, as a critical research problem, has received increasing amounts of attention. To address such issue, the study of individual dynamics, communication topologies and distributed controls plays an important role.

Graph theory contributes significantly to the analysis and synthesis of networked multi-agent systems because it provides general abstractions for how information is shared between agents in a network. Particularly, the graph Laplacian plays an important role in the convergence analysis and has been explored in several contexts [5, 6]. Although the graph Laplacian is a convenient method to describe the geometric interconnection of networked agents, another attractive notion, the edge agreement, which has not been explored extensively, deserves additional attention because the edges are adopted as natural interpretations of the information flow. Pioneering studies on edge agreement protocol provide new insights into how certain subgraphs, such as spanning trees and cycles, affect the convergence properties and set up a novel systematic framework for analyzing multi-agent systems from the edge perspective [7–9]. In these literatures, an important matrix representation is introduced, which is referred to as *edge Laplacian*. The edge agreement in [7] provides a

*Correspondence to: Xiangke Wang, College of Mechatronic Engineering and Automation, National University of Defense Technology, Changsha, 410073, China.
†E-mail: xkwang@nudt.edu.cn

theoretical analysis of the system's performance using both H_2 and H_∞ norms, and these results are applied in relative sensing networks, referring to [8]. Furthermore, based on the properties of the edge Laplacian, Zelazo *et al.* [9] examine how cycles impact the H_2 performance and propose an optimal strategy for designing consensus networks. It is worth noting that, in the aforementioned studies, the edge Laplacian representation is valid for undirected graphs, rather than the more general directed case. Considering the numerous applications of digraphs in multi-agent coordination, extending such a graph tool to the directed case is of great interest.

The information exchange between agents cannot be accurate in practical applications because it is inevitable that types of external noises exist in sensing and transmission, and the existence of perturbations always leads to instability and performance deterioration. Therefore, it is significant to investigate their effects on the behavior of multi-agent systems and design a robust consensus protocol to improve disturbance rejection properties. In [10], the concept of ε-consensus for an undirected graph is introduced in which the state errors are required to converge in a small region under unknown but bounded external disturbances. In the presence of external disturbances, Wen *et al.* [11] guarantee a finite L_2-gain performance under strongly connected graphs. The global consensus with guaranteed H_∞ performance can be achieved under a strongly connected graph in [12], where a Lipschitz continuous multi-agent system subject to external disturbances is considered. Motivated by the aforementioned observations, we consider a more general directed communication graph containing a spanning tree and has unknown but bounded disturbances in the neighbors' state feedback.

Recently, researchers have increasingly been interested in consensus for multi-agent systems with nonlinear dynamics because most of the physical systems are inherently nonlinear in nature. In [13], an adaptive pinning control method is introduced to study the synchronization of uncertain nonlinear networked systems. The second-order consensus of multi-agent systems with heterogeneous nonlinear dynamics and time-varying delays is investigated in [14]. In [15], a distributed control law for the formation tracking of a multi-agent system that is governed by locally Lipschitz continuous dynamics under a directed topology is developed. It should be noted that the studies mentioned earlier are all in the leader–follower setting; however, we will investigate a substantially challenging problem in this paper, that is, the leaderless consensus problem for multi-agent systems with inherently nonlinear dynamics. To the best of our knowledge, most of the existing studies focus on solving the nonlinear leaderless consensus under undirected graphs [16–18], while a few considered the directed topology. Only a small number of studies use the concepts of generalized algebraic connectivity [19], nonsmooth analysis based on the study of Moreau [20], and the limit set-based approach [21] to solve the state agreement problem with nonlinear multi-agent systems under digraphs. However, because of these methods' extremely complicated characters, it is difficult to promote them in the practice. The edge agreement model allows the development of a universal solution framework to address these problems.

To address the technical challenges caused by the external disturbances and the inherently nonlinear dynamics, the concept of input-to-state stability (ISS), which reveals how external inputs affect the internal stability of nonlinear systems (see [22] for a tutorial), is used in this paper. Actually, the concept of ISS is of significance in analyzing large-scale systems, and considerable efforts have been devoted to the interconnected ISS nonlinear systems; particularly, the general cyclic-small-gain theorem of ISS systems developed in [23]. Most recently, the nonlinear small-gain design methods, especially the cyclic-small-gain approach, are utilized to design new distributed control strategies for flocking and containment control in [24] as well as to deal with formation control of nonholonomic mobile robots in [25]. In [26], the authors present a cyclic-small-gain approach to distributed output feedback control of nonlinear multi-agent systems.

This paper initially extends the concept of the edge Laplacian to digraphs and explores its algebraic properties. To proceed with a seamless integration of graph theory and ISS designs, we present a new robust consensus protocol induced from the edge agreement model to solve the leaderless consensus problem with unknown but bounded disturbances and inherently nonlinear dynamics. To better comprehend the edge agreement mechanism, both strongly connected and quasi-strongly connected situations are considered in this paper. The contributions of this paper depend on three aspects. First, the edge Laplacian of digraph is proposed as well as the edge adjacency matrix.

DOI: 10.1002/rnc

Comparing to our previous works [27], much more details about the algebraic properties of the edge Laplacian are explored. As a matter of fact, the invertibility of the incidence matrix and the spectra properties of the edge Laplacian play a central role in the subsequent analysis. Second, we provide a general framework for analyzing the leaderless consensus problem for digraph based on the edge agreement mechanism. Under such framework, the technical challenges caused by the external disturbances and the inherently nonlinear dynamics can be effectively addressed. In particular, we design an integrated procedure for a new robust consensus protocol, which is based on a blend of algebraic graph theory and ISS method. Third, following our setup, the edge-interconnection graph is proposed. One of our primary goals in this paper is to explicitly highlight the insights that the edge-interconnection structure offers in the analysis and synthesis of multi-agent networks. In this direction, we note a reduced-order modeling for the edge agreement in terms of the spanning tree, and based on this observation, a two-subsystem interconnection structure is given.

The organization of this paper is as follows. In Section 2, a brief overview of the basic concepts and results in graph theory is presented as well as the ISS cyclic-small-gain theorem. The edge Laplacian of digraph and other related concepts is proposed in Section 3. The main content on the robust consensus protocol with inherently nonlinear dynamics is elaborated in Section 4. Numerical simulation results are provided in Section 5. The last section presents the conclusions and proposes a number of future research directions.

2. BASIC CONCEPTS AND PRELIMINARY RESULTS

In this section, we present a number of basic concepts in graph theory and the ISS cyclic-small-gain theorem.

2.1. Graph and matrix

In this paper, we use $|\cdot|$ and $\|\cdot\|$ to denote the Euclidean norm and two-norm for vectors and matrices, respectively. The notation $\|\cdot\|_\infty$ is used to denote the supremum norm for a function. Let $\mathcal{R}(A)$ and $\mathcal{N}(A)$ denote the range space and null space of matrix A.

Let $\mathcal{G} = (\mathcal{V}, \mathcal{E}, A_\mathcal{G})$ be a *digraph* of order N with a finite nonempty set of nodes $\mathcal{V} = \{1, 2, \cdots, N\}$, a set of directed edges $\mathcal{E} \subseteq \mathcal{V} \times \mathcal{V}$ with size L, and an adjacency matrix $A_\mathcal{G} = [\alpha_{ij}] \in \mathbb{R}^{N\times N}$, where $\alpha_{ij} = 1$ if and only if $(i, j) \in \varepsilon$ else $\alpha_{ij} = 0$. The degree matrix $\Delta_\mathcal{G} = [\Delta_{ij}]$ is a diagonal matrix with $[\Delta_{ii}] = \sum_{j=1}^{N} \alpha_{ij}, i = 1, 2, \cdots, N$, being the out-degree of node i, and the *graph Laplacian* of the digraph $\mathcal{G}$ is defined by $L_\mathcal{G} = \Delta_\mathcal{G} - A_\mathcal{G}$. For a given parent node i, its incident edge is called the *parent edge* denoted by $\mathcal{P}^i$; its emergent edge is called the *child edge* denoted by $\mathcal{C}^i$; and the edges derived from the same parent i (i.e., the collection of $\mathcal{C}^i$) are called the *sibling edges* denoted by $\mathcal{E}^i_\mathcal{C}$. We call an edge the neighbor of e_k if they share a node, and the neighbor set of e_k is denoted by $N_{e_k} = \{e_l \in \mathcal{E} : \text{if } e_k \text{ and } e_l \text{ share a node}\}$. The *outgoing neighbors* of e_k refer to $N^\otimes_{e_k} = \{e_l \in N_{e_k} : \text{ if } e_k = \mathcal{P}^i \text{ and } e_l = \mathcal{C}^i; \text{ or } e_k, e_l \in \mathcal{E}^i_\mathcal{C}, \text{where } i \text{ is the conjunct node}\}$ (e.g., Figure 1).

A directed path in digraph $\mathcal{G}$ is a sequence of directed edges. A directed tree is a digraph in which, for the root i and any other node j, there exists exactly one directed path from i to j. A spanning tree of a digraph is a directed tree formed by graph edges that connect all the nodes of the graph [28]. Graph $\mathcal{G}$ is called strongly connected if and only if any two distinct nodes can be connected via a directed path and quasi-strongly connected if and only if it has a directed spanning tree [29].

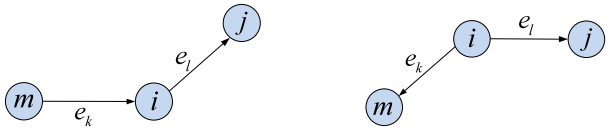

(a) $e_k = \mathcal{P}^i$ and $e_l = \mathcal{C}^i$ (b) $e_k, e_l \in \mathcal{E}^i_\mathcal{C}$

Figure 1. Two typical forms of the outgoing neighbors, $N^\otimes_{e_k}$.

DOI: 10.1002/rnc

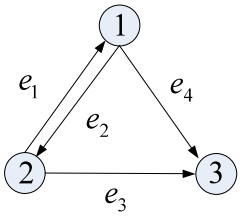

$$E = \begin{bmatrix} -1 & 1 & 0 & 1 \\ 1 & -1 & 1 & 0 \\ 0 & 0 & -1 & -1 \end{bmatrix}$$

Figure 2. The incidence matrix of a simple digraph.

The incidence matrix $E(\mathcal{G})$ for a digraph is a $\{0, \pm 1\}$-matrix with rows and columns indexed by the vertexes and edges of $\mathcal{G}$, respectively, such that

$$[E(\mathcal{G})]_{ik} = \begin{cases} +1 & \text{if } i \text{ is the initial node of edge } e_k, \\ -1 & \text{if } i \text{ is the terminal node of edge } e_k, \\ 0 & \text{otherwise,} \end{cases}$$

which implies that each column of E contains exactly two nonzero entries '$+1$' and '-1'. In addition, for a quasi-strongly connected digraph, the rank of the incidence matrix is $rank(E(\mathcal{G})) = N - 1$ from [29]. Figure 2 depicts an example with its incidence matrix.

2.2. *Input-to-state stability and small-gain theorem*

A function $\alpha : \mathbb{R}_+ \to \mathbb{R}_+$ is said to be *positive definite* if it is continuous, $\alpha(0) = 0$, and $\alpha(s) > 0$ for $s > 0$. A function $\gamma : \mathbb{R}_+ \to \mathbb{R}_+$ is of class $\mathcal{K}$ if it is continuous, strictly increasing, and $\gamma(0) = 0$; it is of class $\mathcal{K}_\infty$ if, in addition, it is unbounded. A function $\beta : \mathbb{R}_+ \times \mathbb{R}_+ \to \mathbb{R}_+$ is of class $\mathcal{KL}$ if, for each fixed t, the function $\beta(\cdot, t)$ is of class $\mathcal{K}$, and for each fixed s, the function $\beta(s, \cdot)$ is decreasing and tends to zero at infinity. Id represents identify function, and symbol $\circ$ denotes the composition between functions.

Consider the following nonlinear system with $x \in \mathbb{R}^n$ as the state and $w \in \mathbb{R}^m$ as the external input

$$\dot{x} = \zeta(x, w), \tag{1}$$

where $\zeta : \mathbb{R}^n \times \mathbb{R}^m \to \mathbb{R}^n$ is a locally Lipschitz vector field.

Definition 1 ([22]*)*
System (1) is said to be *input-to-state stable (ISS)* with w as an input if there exist $\beta \in \mathcal{KL}$ and $\gamma \in \mathcal{K}$ such that for each initial condition $x(0)$ and each measurable essentially bounded input $w(\cdot)$ defined on $[0, \infty)$, the solution $x(\cdot)$ exists on $[0, \infty)$ and satisfies

$$|x(t)| \leqslant \beta(|x(0)|, \gamma(\|w\|_\infty)), \quad \forall t \geqslant 0.$$

It is known that if the system $\dot{x} = f(x, w)$ in (1) is ISS with w as the input, then the unforced system $\dot{x} = f(x, 0)$ is globally asymptotically stable at $x = 0$.

Lemma 1 ([22]*)*
System (1) is ISS if and only if it has an ISS-Lyapunov function.

Consider the following interconnected system composed of N interacting subsystems

$$\dot{x}_i = \zeta_i(x, w_i), \quad i = 1, \ldots, N, \tag{2}$$

where $x_i \in \mathbb{R}^{n_i}$, $w_i \in \mathbb{R}^{m_i}$; and $\zeta_i : \mathbb{R}^{n+m_i} \to \mathbb{R}^{n_i}$ with $n = \sum_{i=1}^N n_i$ is locally Lipschitz continuous such that $x = \left[x_1^T, \ldots, x_N^T\right]^T$ is the unique solution of system (2) for a given initial condition. The external input $w = \left[w_1^T, \ldots, w_N^T\right]^T$ is a measurable and locally essentially bounded function from $\mathbb{R}_+$ to $\mathbb{R}^m$ with $m = \sum_{i=1}^N m_i$. Furthermore, we use $\gamma_y^x \in \mathcal{K}$ to represent the gain function from x-subsystem to y-subsystem [30].

DOI: 10.1002/rnc

Lemma 2 (Cyclic-small-gain Theorem, [23]*)*
Consider the continuous-time dynamical network (2). Suppose that for $i = 1, \ldots, N$, the x_i-subsystem admits an ISS-Lyapunov function $V_i : \mathbb{R}^{n_i} \to \mathbb{R}$ satisfying that

- there exist $\underline{a}_i, \overline{a}_i \in \mathcal{K}_\infty$ such that

$$\underline{a}_i(|x_i|) \leqslant V_i(x_i) \leqslant \overline{a}_i(|x_i|), \quad \forall x_i;$$

- there exist $\gamma_{x_i}^{x_j} \in \mathcal{K} \cup \{0\} (j \neq i)$, $\gamma_{x_i}^{w_i} \in \mathcal{K} \cup \{0\}$ and a positive definite α_i such that

$$V_i(x_i) \geqslant \max\left\{\gamma_{x_i}^{x_j}(V_j(x_j)), \gamma_{x_i}^{w_i}(|w_i|)\right\} \Rightarrow \nabla V_i(x_i)\zeta_i(x, w_i) \leqslant -\alpha_i(V_i(x_i)), \quad \forall x, \ \forall w_i.$$

Then, system (2) is ISS if for each $r = 2, \ldots N$,

$$\gamma_{x_{i_1}}^{x_{i_2}} \circ \gamma_{x_{i_2}}^{x_{i_3}} \circ \cdots \circ \gamma_{x_{i_r}}^{x_{i_1}} < \mathrm{Id} \tag{3}$$

for all $1 \leqslant i_j \leqslant N, i_j \neq i_{j'}$ if $j \neq j'$.

3. THE EDGE LAPLACIAN OF DIGRAPH

The edge Laplacian is a promising graph-theoretic tool; however, it still remains to an undirected notion and is thus inadequate to handle our problem. Undoubtedly, extending the concept of the edge Laplacian to the digraph and exploring its algebraic properties will contribute significantly to the investigation of multi-agent systems. In this section, we first give the definition of the in-incidence and out-incidence matrices.

Remark 1
As known, the 'out-degree' relates how each node in the network impacts on other nodes, but the 'in-degree' directly captures how the dynamics of an agent is influenced by others [31]. In fact, the following investigations, including the definitions and properties, all adopt the 'out-degree' description. However, for the 'in-degree' case, analogous methods can also be applied.

*Definition 2 (*In-incidence *and* out-incidence *matrix)*
The $N \times L$ in-incidence matrix $E_\odot(\mathcal{G})$ for a digraph $\mathcal{G}$ is a $\{0, -1\}$ matrix with rows and columns indexed by nodes and edges of $\mathcal{G}$, respectively, such that

$$[E_\odot(\mathcal{G})]_{ik} := \begin{cases} -1 & \text{if } i \text{ is the terminal node of edge } e_k, \\ 0 & \text{otherwise;} \end{cases}$$

and the out-incidence matrix is a $\{0, +1\}$ matrix, defined as

$$[E_\otimes(\mathcal{G})]_{ik} := \begin{cases} +1 & \text{if } i \text{ is the initial node of edge } e_k, \\ 0 & \text{otherwise.} \end{cases}$$

Comparing with the definition of the incidence matrix, we can write $E(\mathcal{G})$ in the following manner

$$E(\mathcal{G}) = E_\odot(\mathcal{G}) + E_\otimes(\mathcal{G}). \tag{4}$$

In the following discussions, we use E, $E_\odot$, and $E_\otimes$ instead of $E(\mathcal{G})$, $E_\odot(\mathcal{G})$, and $E_\otimes(\mathcal{G})$.

Because each row of the out-incidence matrix actually can be viewed as a decomposition of the out-degree from a node to each specific edge, we can derive a novel factorization of the graph Laplacian.

Lemma 3
Considering a digraph $\mathcal{G}$ with the incidence matrix E and the out-incidence matrix $E_\otimes$, then the graph Laplacian of $\mathcal{G}$ has the following expression:

$$L_\mathcal{G} = E_\otimes E^T. \tag{5}$$

DOI: 10.1002/rnc

Proof
According to the preceding definition of $E_{\otimes}$, we obtain that

$$E_{\otimes i}E_{\otimes j}^T = \begin{cases} [\Delta_{ii}] & \text{if } i = j, \\ 0 & \text{otherwise,} \end{cases}$$

which implies $E_{\otimes}E_{\otimes}^T = \Delta_{\mathcal{G}}$. Similarly, we have

$$E_{\otimes i}E_{\odot j}^T = \begin{cases} -1 & \text{if } j \in N_i, \\ 0 & \text{otherwise,} \end{cases}$$

where N_i denotes the neighbor set of node i, and we can collect the terms as $E_{\otimes}E_{\odot}^T = -A_{\mathcal{G}}$. According to the definition of the graph Laplacian and Equation (4), we have

$$E_{\otimes}E^T = E_{\otimes}E_{\otimes}^T + E_{\otimes}E_{\odot}^T = \Delta_{\mathcal{G}} - A_{\mathcal{G}} = L_{\mathcal{G}}.$$

The proof is concluded. □

Next, we give the definition of the edge variant of the graph Laplacian.

*Definition 3 (*Edge Laplacian of digraph*)*
The edge Laplacian of digraph is defined as

$$L_e := E^T E_{\otimes}$$

with $L \times L$ elements.
*Definition 4 (*Edge-adjacency matrix*)*

$$[A_e]_{kl} := \begin{cases} +1 & e_k, e_l \in \mathcal{E}_{\mathcal{C}}^i, \\ -1 & e_k = \mathcal{P}^i \text{ and } e_l = \mathcal{C}^i, \\ 0 & \text{otherwise.} \end{cases}$$

For instance, the edge Laplacian matrix and the edge-adjacency matrix of the simple digraph shown in Figure 2 are, respectively,

$$L_e = \begin{pmatrix} 1 & -1 & 1 & -1 \\ -1 & 1 & -1 & 1 \\ 1 & 0 & 1 & 0 \\ 0 & 1 & 0 & 1 \end{pmatrix} \text{ and } A_e = \begin{pmatrix} 0 & -1 & 1 & -1 \\ -1 & 0 & -1 & 1 \\ 1 & 0 & 0 & 0 \\ 0 & 1 & 0 & 0 \end{pmatrix}.$$

Lemma 4
The edge Laplacian can be constructed from the edge-adjacency matrix

$$L_e = I + A_e. \tag{6}$$

Proof
According to the definition of $E_{\otimes}$ and A_e, the result comes after the proof of Lemma 3. □

To provide a deeper insight into what the edge Laplacian L_e offers in the analysis and synthesis of multi-agent systems, we propose the following lemma.

Lemma 5
For any digraph $\mathcal{G}$, the graph Laplacian $L_{\mathcal{G}}$ and the edge Laplacian L_e have the same nonzero eigenvalues. In addition, the edge Laplacian L_e contains exactly $N - 1$ nonzero eigenvalues and all in the open right-half plane, if $\mathcal{G}$ is quasi-strongly connected.

DOI: 10.1002/rnc

Proof
Suppose that $\lambda \neq 0$ is an eigenvalue of $L_{\mathcal{G}}$, which is associated with a nonzero eigenvector p. Therefore, we have

$$L_{\mathcal{G}} p = E_{\otimes} E^T p = \lambda p, \tag{7}$$

which implies $E^T p = \bar{p} \neq 0$. By left-multiplying both sides of (7) by E^T, one can obtain

$$L_e \bar{p} = E^T E_{\otimes} E^T p = \lambda \bar{p},$$

which shows that L_e contains the nonzero eigenvalues that $L_{\mathcal{G}}$ has.

By using similar approaches, we can prove that $L_{\mathcal{G}}$ also has all the nonzero eigenvalues of L_e. It turns out that the nonzero eigenvalues of $L_{\mathcal{G}}$ and L_e are identical.

By Lemma 3.3 in [6], for a quasi-strongly connected digraph $\mathcal{G}$ of order N, $L_{\mathcal{G}}$ has $N-1$ nonzero eigenvalues and all in the open right-half plane; therefore, L_e contains exactly $N-1$ nonzero eigenvalues as well. Then we come to the conclusion. □

Lemma 6
Consider a quasi-strongly connected digraph $\mathcal{G}$ of order N, the edge Laplacian L_e has $L - N + 1$ zero eigenvalues, and zero is a simple root of the minimal polynomial of L_e.

Proof
Consider the quasi-strongly connected digraph $\mathcal{G}$, L_e has exactly $N-1$ nonzero eigenvalues; therefore,

$$rank(L_e) \geqslant N - 1, \tag{8}$$

and the algebraic multiplicity of the zero eigenvalue of L_e is $L - N + 1$. Besides, recall the fact that $L_e = E^T E_{\otimes}$ and $rank(E) = N - 1$, so we have

$$rank(L_e) \leqslant rank\left(E^T\right) = N - 1. \tag{9}$$

Then by combining (8) and (9), one can obtain $rank(L_e) = N - 1$, that is, the dimension of the null space of L_e is $dim\, \mathcal{N}(L_e) = L - N + 1$. In other words, the geometric multiplicity of zero eigenvalue is $L - N + 1$. Clearly, the geometric multiplicity and the algebraic multiplicity of zero eigenvalue are equal, which imply that the corresponding Jordan block for each zero eigenvalue is size one from [32]. That is, zero is a simple root of the minimal polynomial of L_e. □

From [33], for the undirected graph, the dynamics of the edge agreement model can be captured by the reduced-order system based on the spanning tree. Next, we will further discuss the similar results under digraph.

Clearly, if the digraph $\mathcal{G}$ is quasi-strongly connected, it can be rewritten as a union form: $\mathcal{G} = \mathcal{G}_{\mathcal{T}} \cup \mathcal{G}_{\mathcal{C}}$, where $\mathcal{G}_{\mathcal{T}}$ is a given spanning tree and $\mathcal{G}_{\mathcal{C}}$ is the co-spanning tree. Correspondingly, the incidence matrix can be rewritten as

$$E = \begin{bmatrix} E_{\mathcal{T}} & E_{\mathcal{C}} \end{bmatrix}$$

through some permutations, and $E_{\mathcal{T}}, E_{\mathcal{C}}$ are incidence matrices with respect to $\mathcal{G}_{\mathcal{T}}$ and $\mathcal{G}_{\mathcal{C}}$. Similarly, the out-incidence matrix can be rewritten as

$$E_{\otimes} = \begin{bmatrix} E_{\otimes\mathcal{T}} & E_{\otimes\mathcal{C}} \end{bmatrix}.$$

It should be mentioned that $\mathcal{G}_{\mathcal{C}}$ can be reconstructed from $\mathcal{G}_{\mathcal{T}}$, which indicates that $E_{\mathcal{T}}$ has full column rank [33].

According to the partition, one can represent the edge Laplacian in terms of the block form of the incidence matrix as

$$L_e = E^T E_{\otimes} = \begin{bmatrix} E_{\mathcal{T}}^T E_{\otimes\mathcal{T}} & E_{\mathcal{T}}^T E_{\otimes\mathcal{C}} \\ E_{\mathcal{C}}^T E_{\otimes\mathcal{T}} & E_{\mathcal{C}}^T E_{\otimes\mathcal{C}} \end{bmatrix} = \begin{bmatrix} L_{e1} & L_{e2} \\ L_{e3} & L_{e4} \end{bmatrix}.$$

DOI: 10.1002/rnc

Also, it is useful to express the edge-adjacency matrix A_e as the block representation

$$A_e = \begin{bmatrix} A_{e1} & A_{e2} \\ A_{e3} & A_{e4} \end{bmatrix}.$$

Following from (6), we have

$$L_{e1} = I_1 + A_{e1},\ L_{e2} = A_{e2},\ L_{e3} = A_{e3},\ \text{and}\ L_{e4} = I_2 + A_{e4}.$$

Lemma 7
Considering a quasi-strongly connected digraph $\mathcal{G} = \mathcal{G}_\mathcal{T} \cup \mathcal{G}_\mathcal{C}$, the pseudoinverse of the incidence matrix $E^\dagger$ exists, and there exists a matrix R such that

$$E^\dagger = R^\dagger E_\mathcal{T}^\dagger \tag{10}$$

with $R^\dagger = R^T \left[RR^T\right]^{-1}$ and $E_\mathcal{T}^\dagger = \left[E_\mathcal{T}^T E_\mathcal{T}\right]^{-1} E_\mathcal{T}^T$, where $R^\dagger$ is the right-inverse of R and $E_\mathcal{T}^\dagger$ is the left inverse of $E_\mathcal{T}$.

Proof
Because $E_\mathcal{T}$ has full column rank, so its left inverse exists and can be directly obtained by $E_\mathcal{T}^\dagger = \left[E_\mathcal{T}^T E_\mathcal{T}\right]^{-1} E_\mathcal{T}^T$. Because the columns of $E_\mathcal{C}$ are linearly dependent on the columns of $E_\mathcal{T}$, we have

$$E_\mathcal{T} T = E_\mathcal{C}, \tag{11}$$

and then the matrix T can be obtained by

$$T = E_\mathcal{T}^\dagger E_\mathcal{C}. \tag{12}$$

The matrix R is now defined as $R = \begin{bmatrix} I & T \end{bmatrix}$. In fact, the rows of the matrix R form a basis for the *cut space* of $\mathcal{G}$ [28]. Besides, the incidence matrix of $\mathcal{G}$ can be written as $E = E_\mathcal{T} R$. Clearly, $E_\mathcal{T}$ is of full column rank and R is of full row rank; therefore, the pseudoinverse of E can be calculated by $E^\dagger = R^\dagger E_\mathcal{T}^\dagger$ from [34]. Then we reach the conclusion. □

4. ROBUST CONSENSUS OF NONLINEAR MULTI-AGENT SYSTEMS VIA INPUT-TO-STATE STABILITY DESIGN

In this section, a new consensus protocol is presented through a seamless integration of graph theory and ISS design. The newly developed cyclic-small-gain theorem is employed to address the challenges caused by unknown but bounded disturbances and the inherently nonlinear dynamics. Contrary to the well-studied graph Laplacian dynamics, we will analyze and synthesize multi-agent systems with the edge perspective by using edge agreement framework. To facilitate a better understanding, both strongly connected and quasi-strongly connected situations are considered.

To begin our analysis, the dynamics of the i-th agent is defined as

$$\dot{x}_i(t) = f\,(t, x_i) + w_i(t) + \mu_i(t), i = 1, 2, \cdots, N, \tag{13}$$

where $x_i(t) \in \mathbb{R}^n$ refers to the state vector of the i-th node; $f\,(t, x_i) : \mathbb{R} \times \mathbb{R}^n \to \mathbb{R}^n$ denotes a Lipschitz continuous function; $w_i(t) \in \mathbb{R}^n$ describes unknown but bounded disturbances with the upper bound $\xi \geqslant 0$, that is, $|w_i(t)| \leqslant \xi$; $\mu_i(t) \in \mathbb{R}^n$ represents the control input.

In the presence of the disturbances, we should not expect that agents can accurately reach consensus. Therefore, we introduce the *robust consensus* to describe the influence of the disturbances on the behavior of the system.

*Definition 5 (*Robust consensus*)*
In the presence of disturbances $w(t)$ with the upper bound ξ, we design a distributed control law $\mu_i(t)$ for $i = 1, 2, \cdots, N$ such that the agent state x_i governed by (13) can reach robust consensus in the nonlinear gain sense that

$$\left|x_i(t) - x_j(t)\right| \leqslant \ell\left(\|w(t)\|_\infty\right),\ \ \ell \in \mathcal{K}\ \ \text{as}\ \ t \to \infty.$$

DOI: 10.1002/rnc

Before proceeding, we make the following assumption.

Assumption 1
For the nonlinear function $f(t, x_i)$ in (13), there exists a non-negative constant η such that

$$|f(t, x_1) - f(t, x_2)| \leqslant \eta |x_1 - x_2|, \forall x_1, x_2 \in \mathbb{R}^n; t \geqslant 0.$$

To reach consensus, we employ the following distributed consensus protocol:

$$\mu_i(t) = -\sum_{j \in N_i} \big(x_i(t) - x_j(t)\big) + u_i(t), i = 1, 2, \cdots, N, \tag{14}$$

where $u_i(t)$ is the auxiliary control input yet to be designed.

4.1. Edge agreement

Considering an edge e_k, we define the *edge state* as $\tilde{x}_{e_k}(t)$, which represents the difference between two agents associated with e_k. We then have

$$\tilde{x}_{e_k}(t) = x_{\otimes(e_k)}(t) - x_{\odot(e_k)}(t), \tag{15}$$

where $\otimes(e_k)$ and $\odot(e_k)$ denote the initial node and the terminal node of e_k, respectively.

Following this, we obtain

$$\tilde{x}_e(t) = E^T x(t), \tag{16}$$

where $\tilde{x}_e(t)$ is the collection of $\tilde{x}_{e_k}(t)$. Consider the well-known graph Laplacian dynamics (linear and noise-free) in [5] as

$$\dot{x}(t) = -Lx(t). \tag{17}$$

Differentiating (16) and substituting in (17) lead to

$$\dot{\tilde{x}}_e(t) = -L_e \tilde{x}_e(t), \tag{18}$$

which is referred to the *edge agreement protocol*. In comparison with the consensus problem, the edge agreement, rather than requiring the convergence to the agreement subspace [5], expects the edge dynamics (18) to converge to the origin. Essentially, the evolution of an edge state depends on its current state and the states of its adjacency edges. In addition, the edge agreement of $\tilde{x}_e$ implies consensus if the digraph $\mathcal{G}$ has a spanning tree [7].

Remark 2
Recall that the objective leaderless consensus is defined as $\lim_{t \to \infty} \big|x_i(t) - x_j(t)\big| = 0$. Obviously, directly modeling such problems is difficult because the coupling of different agents $x_i(t)$ and $x_j(t)$ is involved. However, the edge agreement framework provides a possible method of studying the leaderless consensus problem from the edge perspective. By using (15) and (16), we can turn the consensus problem into an edge agreement problem, where the asymptotic stability of $\tilde{x}_e$ implies the consensus. In fact, based on such framework, the leaderless consensus problem can be extremely simplified. Moreover, we also suggest that the edge agreement does not only provide a broader scope for addressing the leaderless consensus problem but also has a significant potential to address the leader–follower case.

Given protocol (14), the graph Laplacian dynamics is obtained as

$$\dot{x}(t) = \mathcal{F}(t, x) - L_{\mathcal{G}} x(t) + w(t) + u(t), \tag{19}$$

where $\mathcal{F}(t, x)$, $w(t)$ and $\mu(t)$ are the column stack vectors of $f(t, x_i)$, $w_i(t)$, and $\mu_i(t)$, for $i = 1, 2, \cdots, N$.

By differentiating (16) and substituting into (19), we have the following edge Laplacian dynamics:

$$\dot{\tilde{x}}_e(t) = E^T \mathcal{F}(t, x) - L_e \tilde{x}_e(t) + E^T w(t) + E^T u(t), \tag{20}$$

DOI: 10.1002/rnc

where $u(t)$ needs to be further determined. For convenience, we define

$$u_e(t) = E^T u(t). \tag{21}$$

From (6), we have

$$L_{e_k} = 1 + \sum_{e_l \in N_{e_k}^{\otimes}} [A_e]_{kl}.$$

Finally, the state of the k-th edge evolves according to the following system:

$$\dot{\tilde{x}}_{e_k}(t) = f\left(t, x_{\otimes(e_k)}\right) - f\left(t, x_{\odot(e_k)}\right) - \left(\tilde{x}_{e_k}(t) + \sum_{e_l \in N_{e_k}^{\otimes}} [A_e]_{kl} \tilde{x}_{e_l}(t)\right) + \left[E^T\right]_k w(t) + u_{e_k}(t). \tag{22}$$

Remark 3
We use $\mu(t)$ as the only implementable control input for each agent, while we use u_e in the following analysis as a matter of convenience. However, we cannot presume the existence of $u(t)$ because (21) may not have a solution. Actually, whether or not the equation has a solution depends on the topological structure of the graph, and details will be discussed in the next section.

By translating into the edge Laplacian dynamics, the novel system establishes a new control interconnection relation. To describe this relationship, we provide the following definition.

*Definition 6 (*Edge-interconnection digraph*)*
Considering the $\tilde{x}_{e_k}$-subsystems as nodes and the control interconnections as directed edges, the interconnected system composed of the $\tilde{x}_{e_k}$-subsystems can be modeled as a digraph $\tilde{\mathcal{G}}$ called *edge-interconnection digraph*.

In fact, $\tilde{\mathcal{G}}$ can be easily constructed from $\mathcal{G}$, and Equation (22) illustrates the connection of the edge-interconnection digraph. In particular, there are two steps to transform $\mathcal{G}$ into $\tilde{\mathcal{G}}$. First, all the edges e_k in $\mathcal{G}$ are modeled as the vertices and denoted by π_k. Second, base on (22) and the definition of A_e, for any specified edge pair e_k, e_l, if $e_k, e_l \in \mathcal{E}_{\mathcal{C}}^i$, then π_k and π_l are connected by a bidirectional edge; and if $e_k = \mathcal{P}^i$ and $e_l = \mathcal{C}^i$, there will be a directed edge incident into π_k from π_l. Figure 3 depicts the corresponding edge-interconnection digraph of the example shown in Figure 2. To reveal the intricate relation between the original digraph and the edge-interconnection digraph, we need the following lemma.

Lemma 8
For a rooted tree, the corresponding edge-interconnection digraph $\tilde{\mathcal{G}}$ is composed of several strongly connected subgraphs $\tilde{\mathcal{G}}_i, i = 1, 2, \cdots$, which are coupled through simple cascaded connections and parallel connections.

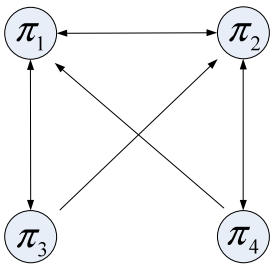

Figure 3. The corresponding edge-interconnection digraph of Figure 2.

DOI: 10.1002/rnc

Proof
Obviously, the sibling edges $\mathcal{E}_{\mathcal{C}}^{i}$ with the same parent i form a strongly connected components in the edge-interconnection digraph, because they affect each other mutually. Besides, for the $e_k = \mathcal{P}^i$, and $e_l = \mathcal{C}^i$, there will be a directed edge incident into π_k from π_l which forms the cascaded connection in the same branch. When taking the strongly connected components as nodes, $\tilde{\mathcal{G}}$ is acyclic and consists of several cascaded connections and parallel connections. For instance, consider a rooted tree in Figure 4(a), the corresponding edge-interconnection digraph is illustrated in Figure 4(b). □

Lemma 9
The edge-interconnection graph $\tilde{\mathcal{G}}$ is strongly connected if and only if $\mathcal{G}$ is strongly connected digraph.

Proof
Clearly, for the strongly connected graph, there will be a directed path connecting any pair of edges (e_k, e_l) in each direction. In that way, any two distinct nodes (π_k, π_l) of $\tilde{\mathcal{G}}$ can be connected via a directed path; therefore, $\tilde{\mathcal{G}}$ is strongly connected. On the other hand, while $\tilde{\mathcal{G}}$ is strongly connected, it implies that, for any pair of nodes of $\mathcal{G}$, there always exists a directed path connecting them, that is, $\mathcal{G}$ is also strongly connected. □

4.2. *Main results*

In this section, both strongly connected digraphs and quasi-strongly connected digraphs are considered. The cyclic-small-gain theorem is then employed to guarantee the robust consensus of the closed-loop multi-agent systems. Note that ISS cyclic-small-gain theorem can be directly applied if the underlying digraph is strongly connected from [23]. However, for the quasi-strongly case, we will translate it into a two-subsystem interconnection structure.

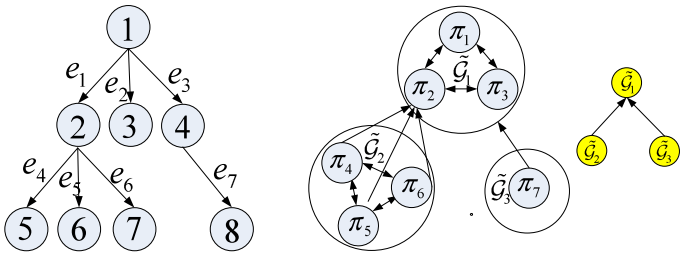

(a) A simple rooted tree. (b) The edge-interconnection digraph.

Figure 4. The corresponding edge-interconnection digraph with three strongly connected components $\tilde{\mathcal{G}}_1$, $\tilde{\mathcal{G}}_2$, and $\tilde{\mathcal{G}}_3$.

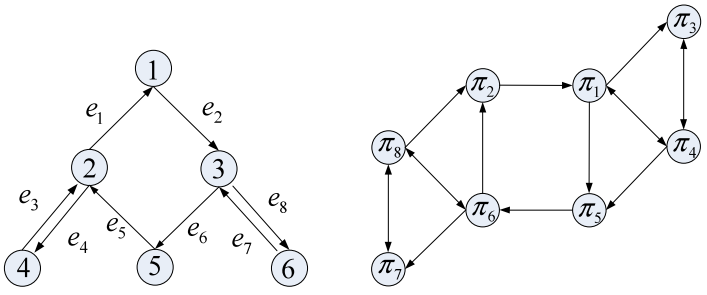

(a) The strongly connected digraph. (b) The edge-interconnection digraph.

Figure 5. The original strongly connected digraph and the corresponding edge-interconnection digraph.

DOI: 10.1002/rnc

4.2.1. Strongly connected digraph. A digraph $\mathcal{G}$ of a six-agent system is shown as an example in Figure 5(a), and the corresponding edge-interconnection digraph is shown in Figure 5(b). From Lemma 9, we know that the edge-interconnection digraph is strongly connected if $\mathcal{G}$ is strongly connected.

To begin our analysis, we define the following ISS-Lyapunov function candidate

$$V_{e_k} = \frac{1}{2}\tilde{x}_{e_k}^T \tilde{x}_{e_k}, \;\; k = 1, 2, \cdots, L;$$

and we denote Θ as the set of all simple loops (for more details, please refer to [23]) of $\mathcal{G}$, and $A_o(\gamma_{\tilde{x}_{e_k}}^{\tilde{x}_{e_l}})$ as the product of the gain assigned to the edges of a simple loop $o \in \Theta$, where $\gamma_{\tilde{x}_{e_k}}^{\tilde{x}_{e_l}} \in K_\infty$ with $k = 1, 2, \cdots L$ and $e_l \in N_{e_k}^{\otimes}$.

The main result for the strongly connected digraph is given as follows.

Theorem 1

Assuming that the digraph is strongly connected, consider subsystem (22) with $\tilde{x}_{e_k}$ as the state, and $\tilde{x}_{e_l}\left(e_l \in N_{e_k}^{\otimes}\right)$ as the external inputs. For any specified constant σ_{e_k} and $\gamma_{\tilde{x}_{e_k}}^{\tilde{x}_{e_l}} \in K_\infty \left(e_l \in N_{e_k}^{\otimes}\right)$, we can design

$$u_{e_k} = -\frac{\tilde{x}_{e_k}}{\left|\tilde{x}_{e_k}\right|}\left[\eta\left|\tilde{x}_{e_k}\right| + \sum_{e_l \in N_{e_k}^{\otimes}} |[A_e]_{kl}| \rho_{\tilde{x}_{e_l}}^{\tilde{x}_{e_k}}\left(\left|\tilde{x}_{e_k}\right|\right) + \sqrt{2}\xi\right] + \left(1 - \frac{\sigma_{e_k}}{2}\right)\tilde{x}_{e_k} \tag{23}$$

with $\rho_{\tilde{x}_{e_l}}^{\tilde{x}_{e_k}} = \underline{\alpha}^{-1} \circ \left(\gamma_{\tilde{x}_{e_k}}^{\tilde{x}_{e_l}}\right)^{-1} \circ \overline{\alpha}(s)$ such that subsystem (22) is ISS with ISS-Lyapunov function V_{e_k} satisfying

$$V_{e_k} \geqslant \max_{e_l \in N_{e_k}^{\otimes}} \left\{\gamma_{\tilde{x}_{e_k}}^{\tilde{x}_{e_l}}\left(V_{e_l}\right)\right\} \Rightarrow \nabla V_{e_k} \dot{\tilde{x}}_{e_k} \leqslant -\sigma_{e_k} V_{e_k}.$$

If the required cyclic-small-gain condition (3) is satisfied, the composed system is ISS. Then, the objective robust consensus can be achieved by using the distributed consensus protocol (14) with

$$\mathrm{u} = [E^T]^{\dagger} u_e. \tag{24}$$

Proof

Because $V_{e_k} \geqslant \max_{e_l \in N_{e_k}^{\otimes}} \left\{\gamma_{\tilde{x}_{e_k}}^{\tilde{x}_{e_l}}\left(V_{e_l}\right)\right\}$, we have

$$\left|\tilde{x}_{e_l}\right| \leqslant \rho_{\tilde{x}_{e_l}}^{\tilde{x}_{e_k}}\left(\left|\tilde{x}_{e_k}\right|\right), e_l \in N_{e_k}^{\otimes}.$$

Note that $\left|\left[E^T\right]_k\right| = \sqrt{2}$ and by taking the derivative of V_{e_k}, we have

$$\begin{aligned}
\nabla V_{e_k} \dot{\tilde{x}}_{e_k} &= \tilde{x}_{e_k}^T \dot{\tilde{x}}_{e_k} \\
&= \tilde{x}_{e_k}^T \left[u_{e_k} + \left(f\left(t, x_{\otimes(e_k)}\right) - f\left(t, x_{\odot(e_k)}\right)\right) + [E^T]_k w - \left(\tilde{x}_{e_k} + \sum_{e_l \in N_{e_k}^{\otimes}} [A_e]_{kl} \tilde{x}_{e_l}\right)\right] \\
&\leqslant \tilde{x}_{e_k}^T \left(u_{e_k} - \tilde{x}_{e_k}\right) + \eta\left|\tilde{x}_{e_k}^T\right|\left|\tilde{x}_{e_k}\right| + \sqrt{2}\xi\left|\tilde{x}_{e_k}^T\right| - \tilde{x}_{e_k}^T \sum_{e_l \in N_{e_k}^{\otimes}} [A_e]_{kl} \tilde{x}_{e_l} \\
&\leqslant \tilde{x}_{e_k}^T \left(u_{e_k} - \tilde{x}_{e_k}\right) + \eta\left|\tilde{x}_{e_k}^T\right|\left|\tilde{x}_{e_k}\right| + \sqrt{2}\xi\left|\tilde{x}_{e_k}^T\right| + \left|\tilde{x}_{e_k}^T\right| \sum_{e_l \in N_{e_k}^{\otimes}} |[A_e]_{kl}| \rho_{\tilde{x}_{e_l}}^{\tilde{x}_{e_k}}\left(\left|\tilde{x}_{e_k}\right|\right).
\end{aligned}$$

DOI: 10.1002/rnc

Using (23), we have

$$\nabla V_{e_k} \dot{\tilde{x}}_{e_k} \leqslant -\frac{\sigma_{e_k}}{2} \tilde{x}_{e_k}^T \tilde{x}_{e_k} = -\sigma_{e_k} V_{e_k},$$

which implies that the $\tilde{x}_k$-subsystem is ISS.

Because the induced edge-interconnection digraph is strongly connected, the ISS cyclic-small-gain theorem can be directly implemented. If the following cyclic-small-gain condition is satisfied

$$A_o \left(\gamma_{\tilde{x}_{e_k}}^{\tilde{x}_{e_l}} \right) < \mathrm{Id},$$

then the composed system (20) is ISS.

It should be mentioned that as u_e is designed, the whole system $\tilde{x}_e(t)$ is unforced. Based on the ISS property, we have

$$|\tilde{x}_e(t)| \leqslant \tilde{\beta} \left(\left| \tilde{x}^0 \right|, t \right) + \tilde{\gamma} \left(\|w\|_\infty \right), t \geqslant 0$$

where $\tilde{x_e^0}$ is the initial state of $\tilde{x}_e(t)$ and $\tilde{\beta} \in \mathcal{KL}$, $\tilde{\gamma} \in \mathcal{K}$. Obviously, as $t \to \infty$, we have $\tilde{\beta} \left(\left| \tilde{x}^0 \right|, t \right) = 0$. So that

$$\lim_{t \to \infty} |\tilde{x}_e(t)| \leqslant \tilde{\gamma} \left(\|w\|_\infty \right),$$

which implies the robust consensus. Because $\mathcal{G}$ has a spanning tree, the pseudoinverse $[E^T]^\dagger$ exists. Then we can obtain the implemented consensus control input by using (24). The proof is concluded. □

4.2.2. Quasi-strongly connected digraph. In this section, we consider a quasi-strongly connected digraph $\mathcal{G} = \mathcal{G}_\mathcal{T} \cup \mathcal{G}_\mathcal{C}$. An example is given as Figure 6(a). The edges of $\mathcal{G}_\mathcal{T}$ are marked as red. Accordingly, the edge-interconnection digraph is shown in Figure 6(b), which consists of two parts: $\tilde{\mathcal{G}} = \tilde{\mathcal{G}}_\mathcal{T} \cup \tilde{\mathcal{G}}_\mathcal{C}$. Correspondingly, the edge Laplacian dynamics system $\tilde{x}_e(t)$ can be modeled as the interconnection of the $H_\mathcal{T}$-subsystem and the $H_\mathcal{C}$-subsystem based on $\tilde{\mathcal{G}}_\mathcal{T}$ and $\tilde{\mathcal{G}}_\mathcal{C}$.

As previously mentioned, the incidence matrix can be rewritten as $E = \begin{bmatrix} E_\mathcal{T} & E_\mathcal{C} \end{bmatrix}$, and the edge Laplacian can be represented as the block form $L_e = \begin{bmatrix} L_{e1} & L_{e2} \\ L_{e3} & L_{e4} \end{bmatrix}$ in line with the permutation. Therefore, the edge Laplacian dynamics $\tilde{x}_e(t)$ described by (20) can be translated into the following form:

$$H_\mathcal{T} : \dot{\tilde{x}}_\mathcal{T}(t) = \mathcal{F}_\mathcal{T}(t, x) - L_{e_1} \tilde{x}_\mathcal{T}(t) - L_{e_2} \tilde{x}_\mathcal{C}(t) + E_\mathcal{T}^T w(t) + u_\mathcal{T}(t)$$

with $\mathcal{F}_\mathcal{T}(t, x) = E_\mathcal{T}^T \mathcal{F}(t, x)$, $u_\mathcal{T}(t) = E_\mathcal{T}^T u(t)$.

$$H_\mathcal{C} : \dot{\tilde{x}}_\mathcal{C}(t) = \mathcal{F}_\mathcal{C}(t, x) - L_{e_4} \tilde{x}_\mathcal{C}(t) - L_{e_3} \tilde{x}_\mathcal{T}(t) + E_\mathcal{C}^T w(t) + u_\mathcal{C}(t)$$

with $\mathcal{F}_\mathcal{C}(t, x) = E_\mathcal{T}^T \mathcal{F}(t, x)$, $u_\mathcal{C}(t) = E_\mathcal{C}^T u(t)$. Besides, $E_\mathcal{T}^T w$ and $E_\mathcal{C}^T w$ indicate unknown but bounded disturbances on $\tilde{\mathcal{G}}_\mathcal{T}$ and $\tilde{\mathcal{G}}_\mathcal{C}$, respectively. The interacting system is shown in Figure 7.

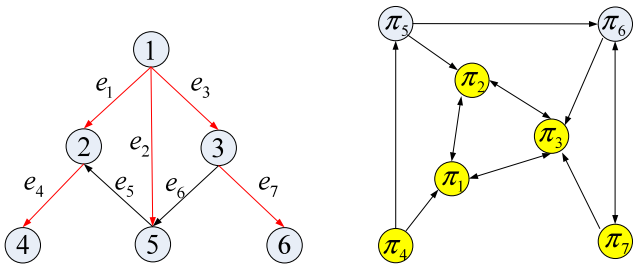

(a) The quasi-strongly connected digraph. (b) The edge-interconnection digraph.

Figure 6. The quasi-strongly connected digraph and the corresponding edge-interconnection digraph.

DOI: 10.1002/rnc

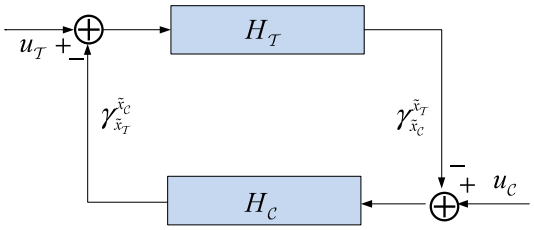

Figure 7. The interconnection of subsystems H_t and H_c.

Obviously, for a specific spanning tree, it contains $N-1$ edges. For subsystem $\tilde{x}_{\mathcal{T}_k}$, with $k = 1, 2, \cdots, N-1$, $e_l, e_k \in \mathcal{G}_{\mathcal{T}}$, we have

$$\dot{\tilde{x}}_{\mathcal{T}_k} = F_{\mathcal{T}_k} - \left(\tilde{x}_{\mathcal{T}_k} + \sum_{e_l \in N^{\otimes}_{e_k}} \left[A_{e_1}\right]_{kl} \tilde{x}_{\mathcal{T}_l} \right) - Le_{2_k} \tilde{x}_{\mathcal{C}} + \left[E^T_{\mathcal{T}}\right]_k w + u_{\mathcal{T}_k}. \tag{25}$$

We choose the following ISS-Lyapunov candidates:

$$V_{\mathcal{T}_k} = \frac{1}{2} \tilde{x}^T_{\mathcal{T}_k} \tilde{x}_{\mathcal{T}_k}, \quad k = 1, 2, \cdots, N-1, \tag{26}$$

$$V_{\mathcal{T}} = \frac{1}{2} \tilde{x}^T_{\mathcal{T}} \tilde{x}_{\mathcal{T}}, \tag{27}$$

$$V_{\mathcal{C}} = \frac{1}{2} \tilde{x}^T_{\mathcal{C}} \tilde{x}_{\mathcal{C}}. \tag{28}$$

Denote $\Theta_{\mathcal{T}}$ as the set of all the simple loops of $\tilde{\mathcal{G}}_{\mathcal{T}}$, and denote $A_{\mathcal{T}_o}(\gamma^{\tilde{x}_{t_l}}_{\tilde{x}_{t_k}})$ as the product of the gain assigned to the edges of a simple loop in $\Theta_{\mathcal{T}}$. Let $\bar{\lambda}_1$ denote the smallest nonzero eigenvalue of matrix TT^T, where T is defined in (12).

We then present the main result for the quasi-strongly connected digraph as follows.

Theorem 2

Assuming that the digraph is quasi-strongly connected, consider subsystem (25) with $\tilde{x}_{\mathcal{T}_k}$ $(e_k \in \mathcal{G}_{\mathcal{T}})$ as the internal state. Let $\tilde{x}_{\mathcal{T}_l}$ $\left(e_l \in N^{\otimes}_{e_k} \cap \mathcal{G}_{\mathcal{T}}\right)$ and $\tilde{x}_{\mathcal{C}}$ $(e_c \in \mathcal{G}_{\mathcal{C}})$ be the external inputs. For any specified constant $\sigma_{\mathcal{T}_k} > 0$ and $\gamma^{\tilde{x}_{\mathcal{T}_l}}_{\tilde{x}_{\mathcal{T}_k}}, \gamma^{\tilde{x}_{\mathcal{C}}}_{\tilde{x}_{\mathcal{T}_k}} \in k_\infty$, we can design

$$\begin{aligned} u_{\mathcal{T}_k} = &-\frac{\tilde{x}_{\mathcal{T}_k}}{\left|\tilde{x}_{\mathcal{T}_k}\right|} \left[\eta \left|\tilde{x}_{\mathcal{T}_k}\right| + \sum_{e_l \in N^{\otimes}_{e_k}} \left|\left[A_{e_1}\right]_{kl}\right| \rho^{\tilde{x}_{\mathcal{T}_k}}_{\tilde{x}_{\mathcal{T}_l}} \left(\left|\tilde{x}_{\mathcal{T}_k}\right|\right) + \left|L_{e_{2k}}\right| \rho^{\tilde{x}_{\mathcal{T}_k}}_{\tilde{x}_{\mathcal{C}}} \left(\left|\tilde{x}_{\mathcal{T}_k}\right|\right) + \sqrt{2}\xi \right] \\ &+ \left(1 - \frac{\sigma_{\mathcal{T}_k}}{2}\right) \tilde{x}_{\mathcal{T}_k} \end{aligned} \tag{29}$$

with $\rho^{\tilde{x}_{\mathcal{T}_k}}_{\tilde{x}_{\mathcal{T}_l}} = \underline{\alpha}^{-1} \circ \left(\gamma^{\tilde{x}_{\mathcal{T}_l}}_{\tilde{x}_{\mathcal{T}_k}}\right)^{-1} \circ \overline{\alpha}(s)$ and $\rho^{\tilde{x}_{\mathcal{T}_k}}_{\tilde{x}_{\mathcal{C}}} = \underline{\alpha}^{-1} \circ \left(\gamma^{\tilde{x}_{\mathcal{C}}}_{\tilde{x}_{\mathcal{T}_k}}\right)^{-1} \circ \overline{\alpha}(s)$, such that the subsystem (25) is ISS with an ISS-Lyapunov function $V_{\mathcal{T}_k}$ satisfying

$$V_{\mathcal{T}_k} \geqslant \max_{e_l \in N^{\otimes}_{e_k}} \left\{ \gamma^{\tilde{x}_{\mathcal{T}_l}}_{\tilde{x}_{\mathcal{T}_k}} \left(V_{\mathcal{T}_l}\right), \gamma^{\tilde{x}_{\mathcal{C}}}_{\tilde{x}_{\mathcal{T}_k}} \left(V_{\mathcal{C}}\right) \right\} \Rightarrow \nabla V_{\mathcal{T}_k} \dot{\tilde{x}}_{\mathcal{T}_k} \leqslant -\sigma_{\mathcal{T}_k} V_{\mathcal{T}_k}.$$

DOI: 10.1002/rnc

If the cyclic-small-gain condition (3) as well as

$$\gamma_{\tilde{x}_{\mathcal{T}_k}}^{\tilde{x}_{\mathcal{C}}} < \frac{1}{\bar{\lambda}_1 (N-1)} \tag{30}$$

are satisfied, the whole system is ISS. Then the objective robust consensus can be achieved by using protocol (14) with

$$\mathrm{u} = \left[E_{\mathcal{T}}^T\right]^{\dagger} u_{\mathcal{T}}. \tag{31}$$

Proof

The main proof procedure contains three steps. First, for the $\tilde{x}_{\mathcal{T}_k}$-subsystem, the ISS properties can be guaranteed by taking (29) as the control law. Second, the ISS properties of the upside subsystem $H_{\mathcal{T}}$ are then proven by utilizing the ISS cyclic-small-gain theorem. Finally, we prove that the downside subsystem $H_{\mathcal{C}}$ is ISS, and the objective robust consensus can be achieved while the small gain condition $\gamma_{\tilde{x}_{\mathcal{T}}}^{\tilde{x}_{\mathcal{C}}} \circ \gamma_{\tilde{x}_{\mathcal{C}}}^{\tilde{x}_{\mathcal{T}}} < \mathrm{Id}$ is satisfied.

Step 1: Using the Lyapunov candidate defined in (26) and considering $V_{\mathcal{T}_k} \geqslant \max_{e_l \in N_{e_k}^{\otimes}} \left\{\gamma_{\tilde{x}_{\mathcal{T}_k}}^{\tilde{x}_{\mathcal{T}_l}}\left(V_{\mathcal{T}_l}\right), \gamma_{\tilde{x}_{\mathcal{T}_k}}^{\tilde{x}_{\mathcal{C}}}\left(V_{\mathcal{C}}\right)\right\}$ with $e_l, e_k \in \mathcal{G}_{\mathcal{T}}, e_c \in \mathcal{G}_{\mathcal{C}}$, we have

$$\begin{aligned} |\tilde{x}_{\mathcal{C}}| &\leqslant \rho_{\tilde{x}_{\mathcal{C}}}^{\tilde{x}_{\mathcal{T}_k}}\left(\left|\tilde{x}_{\mathcal{T}_k}\right|\right), \\ \left|\tilde{x}_{\mathcal{T}_l}\right| &\leqslant \rho_{\tilde{x}_{\mathcal{T}_l}}^{\tilde{x}_{\mathcal{T}_k}}\left(\left|\tilde{x}_{\mathcal{T}_k}\right|\right). \end{aligned}$$

Taking the derivative of $V_{\mathcal{T}_k}$, we have

$$\begin{aligned} \nabla V_{\mathcal{T}_k} \dot{\tilde{x}}_{\mathcal{T}_k} = \tilde{x}_{\mathcal{T}_k}^T \dot{\tilde{x}}_{\mathcal{T}_k} = \tilde{x}_{\mathcal{T}_k}^T \Bigg[& u_{\mathcal{T}_k} + f\left(t, x_{\otimes(e_k)}\right) - f\left(t, x_{\odot(e_k)}\right) \\ & - \left(\tilde{x}_{\mathcal{T}_k} + \sum_{e_l \in N_{e_k}^{\otimes}} \left[A_{e_1}\right]_{kl} \tilde{x}_{\mathcal{T}_l}\right) - L e_{2_k} \tilde{x}_{\mathcal{C}} + \left[E_{\mathcal{T}}^T\right]_k w \Bigg] \\ \leqslant \tilde{x}_{\mathcal{T}_k}^T \left(u_{\mathcal{T}_k} - \tilde{x}_{\mathcal{T}_k}\right) + \eta \left|\tilde{x}_{\mathcal{T}_k}^T\right| \left|\tilde{x}_{\mathcal{T}_k}\right| - \tilde{x}_{\mathcal{T}_k}^T \sum_{e_l \in N_{e_k}^{\otimes}} \left[A_{e_1}\right]_{kl} \tilde{x}_{\mathcal{T}_l} - \tilde{x}_{\mathcal{T}_k}^T L e_{2_k} \tilde{x}_{\mathcal{C}} \\ + \tilde{x}_{\mathcal{T}_k}^T \left[E_{\mathcal{T}}^T\right]_k w \leqslant \tilde{x}_{\mathcal{T}_k}^T \left(u_{\mathcal{T}_k} - \tilde{x}_{\mathcal{T}_k}\right) + \eta \left|\tilde{x}_{\mathcal{T}_k}^T\right| \left|\tilde{x}_{\mathcal{T}_k}\right| \\ + \left|\tilde{x}_{\mathcal{T}_k}^T\right| \sum_{e_l \in N_{e_k}^{\otimes}} \left|\left[A_{e_1}\right]_{kl}\right| \rho_{\tilde{x}_{\mathcal{T}_l}}^{\tilde{x}_{\mathcal{T}_k}}\left(\left|\tilde{x}_{\mathcal{T}_k}\right|\right) + \left|\tilde{x}_{\mathcal{T}_k}^T\right| \left|L_{e_{2k}}\right| \rho_{\tilde{x}_{\mathcal{C}}}^{\tilde{x}_{\mathcal{T}_k}}\left(\left|\tilde{x}_{\mathcal{T}_k}\right|\right) \\ + \sqrt{2}\xi \left|\tilde{x}_{\mathcal{T}_k}^T\right|. \end{aligned}$$

By using (29), we obtain

$$\nabla V_{\mathcal{T}_k} \dot{\tilde{x}}_{\mathcal{T}_k} \leqslant -\frac{\sigma_{\mathcal{T}_k}}{2} \tilde{x}_{\mathcal{T}_k}^T \tilde{x}_{\mathcal{T}_k} = -\sigma_{\mathcal{T}_k} V_{\mathcal{T}_k},$$

which implies that the $\tilde{x}_{\mathcal{T}_k}$-subsystem is ISS.

Step 2: We define $\tilde{x}_{s_i} = \{\tilde{x}_{\mathcal{T}_k} : e_k \in \tilde{\mathcal{G}}_{\mathcal{T}} \text{ and } e_k \in \mathcal{E}_{\mathcal{C}}^i\}$ as the state of the strongly connected component. By taking (29) as the input, each subsystem $\tilde{x}_{\mathcal{T}_k}$ is ISS and admits an ISS-Lyapunov function $V_{\mathcal{T}_k}$. From Lemma 2, for the set of all the simple loops $\Theta_{\mathcal{T}}$, if the cyclic-small-gain condition

$$A_{\mathcal{T}_o}\left(\gamma_{\tilde{x}_{\mathcal{T}_k}}^{\tilde{x}_{\mathcal{T}_l}}\right) < \mathrm{Id}$$

DOI: 10.1002/rnc

is satisfied, then the composed subsystem $\tilde{x}_{s_i}$ is ISS. By taking the strongly connected subsystems $\tilde{x}_{s_i}$ as nodes, the upside subsystem $H_{\mathcal{T}}$ is acyclic as we previously mentioned in Lemma 8. From [35], we note that the ISS properties are retained if the underlying digraph is acyclic. Therefore, the upside subsystem $H_{\mathcal{T}}$ is ISS as well.

Additionally, we can verify that $V_{\mathcal{T}}$ defined in (27) is an ISS-Lyapunov function. Also, we can calculate the interconnection gain $\gamma_{\tilde{x}_{\mathcal{T}}}^{\tilde{x}_{\mathcal{C}}}$ from $H_{\mathcal{C}}$ to $H_{\mathcal{T}}$. To begin with, according to

$$V_{\mathcal{T}_k} \geqslant \max_{e_l \in N_{e_k}^{\otimes}} \left\{ \gamma_{\tilde{x}_{\mathcal{T}_k}}^{\tilde{x}_{\mathcal{T}_l}} \left(V_{\mathcal{T}_l} \right), \gamma_{\tilde{x}_{\mathcal{T}_k}}^{\tilde{x}_{\mathcal{C}}} \left(V_{\mathcal{C}} \right) \right\},$$

we have

$$V_{\mathcal{T}} \geqslant (N-1)\gamma_{\tilde{x}_{\mathcal{T}_k}}^{\tilde{x}_{\mathcal{C}}} \left(V_{\mathcal{C}} \right), k = 1, 2, \cdots, N-1$$

because $V_{\mathcal{T}} = \sum_{k=1}^{N-1} V_{\mathcal{T}_k}$.

By choosing $\sigma_k = \sigma > 0$, we obtain

$$\nabla V_{\mathcal{T}} \dot{\tilde{x}}_{\mathcal{T}} = \sum_{k=1}^{N-1} \nabla V_{\mathcal{T}_k} \dot{\tilde{x}}_{\mathcal{T}_k} \leqslant -\sum_{k=1}^{N-1} \frac{\sigma_k}{2} \tilde{x}_{\mathcal{T}_k}^T \tilde{x}_{\mathcal{T}_k} = -\sigma V_{\mathcal{T}},$$

which implies that $V_{\mathcal{T}_k}$ is an ISS-Lyapunov function. Then we can simply choose $\gamma_{\tilde{x}_{\mathcal{T}}}^{\tilde{x}_{\mathcal{C}}}$ as

$$\gamma_{\tilde{x}_{\mathcal{T}}}^{\tilde{x}_{\mathcal{C}}} = (N-1)\gamma_{\tilde{x}_{\mathcal{T}_k}}^{\tilde{x}_{\mathcal{C}}}. \tag{32}$$

Step 3: Because we have $\tilde{x}_{\mathcal{C}} = T^T \tilde{x}_{\mathcal{T}}$ from (11), then

$$V_{\mathcal{C}} = \frac{1}{2} \tilde{x}_{\mathcal{C}}^T \tilde{x}_{\mathcal{C}} = \frac{1}{2} \tilde{x}_{\mathcal{T}}^T T T^T \tilde{x}_{\mathcal{T}},$$

where $T T^T$ is symmetric positive semidefinite. Suppose the eigenvalues of $T T^T$ can be ordered and denoted as $0 \leqslant \bar{\lambda}_1 \leqslant \bar{\lambda}_2 \leqslant \cdots \leqslant \bar{\lambda}_{N-1}$. Clearly, one can obtain that $V_{\mathcal{C}} \geqslant \bar{\lambda}_1 V_{\mathcal{T}}$.

Assume that P is an orthogonal transformation matrix and let $\tilde{x}_{\mathcal{T}} = P y$, then we can translate $V_{\mathcal{C}}$ into a standard quadratic form as follows:

$$V_{\mathcal{C}} = \frac{1}{2} \left(\bar{\lambda}_1 y_1^2 + \bar{\lambda}_2 y_2^2 + \cdots + \bar{\lambda}_{N-1} y_{N-1}^2 \right).$$

By taking the derivation of $V_{\mathcal{C}}$, one can obtain

$$\begin{aligned} \nabla V_{\mathcal{C}} \dot{\tilde{x}}_{\mathcal{C}} &= \sum_{k=1}^{N-1} \bar{\lambda}_k y_k^T \dot{y}_k = \sum_{k=1}^{N-1} \bar{\lambda}_k \tilde{x}_{\mathcal{T}}^T P_k P_k^{-1} \dot{\tilde{x}}_{\mathcal{T}} \\ &= \sum_{k=1}^{N-1} \bar{\lambda}_k \nabla V_{\mathcal{T}} \dot{\tilde{x}}_{\mathcal{T}} \leqslant -\sigma \sum_{k=1}^{N-1} \bar{\lambda}_k V_{\mathcal{T}} \leqslant -\frac{\sigma}{\bar{\lambda}_{N-1}} \sum_{k=1}^{N-1} \bar{\lambda}_k V_{\mathcal{C}}, \end{aligned}$$

which implies that $V_{\mathcal{C}}$ is an ISS-Lyapunov function. Then we can choose the interconnection gain as

$$\gamma_{\tilde{x}_{\mathcal{C}}}^{\tilde{x}_{\mathcal{T}}} = \bar{\lambda}_1. \tag{33}$$

DOI: 10.1002/rnc

For this two interacting subsystems $H_{\mathcal{T}}$ and $H_{\mathcal{C}}$, if the small gain condition $\gamma_{\tilde{x}_{\mathcal{T}}}^{\tilde{x}_{\mathcal{C}}} \circ \gamma_{\tilde{x}_{\mathcal{C}}}^{\tilde{x}_{\mathcal{T}}} < \mathrm{Id}$ holds, then the whole system is ISS. To satisfy the small gain condition, by combining (32) and (33), we can choose

$$\gamma_{\tilde{x}_{\mathcal{T}_k}}^{\tilde{x}_{\mathcal{C}}} < \frac{1}{\bar{\lambda}_1 (N-1)}. \tag{34}$$

From Theorem 1, it is clear that the objective robust consensus can be guaranteed while (34) holds. □

Remark 4

The ISS-Lyapunov function for the composite system $\tilde{x}(t)$ can be obtained by using the approach mentioned in [23]. Besides, the discussion about the explicit cyclic-small-gain conditions required in (3) can be found in our previous study [36]. In particular, we can check that the cyclic-small-gain conditions can be guaranteed by simply choosing the nonlinear gains $\gamma_{\tilde{x}_{e_k}}^{\tilde{x}_{e_l}} < \mathrm{Id}$, with $e_l \in N_{e_k}^{\otimes}$.

5. SIMULATIONS

Numerical simulations are performed to illustrate the obtained theoretical results. For this set of simulations, we consider a six-agent system with both strongly connected graph and quasi-strongly connected graph. The dynamics of the i-th agent is assumed to be

$$\dot{x}_i(t) = f(t, x_i) + w_i(t) + u_i(t), \quad i = 1, 2, \cdots, 6,$$

where $x_i(t), u_i(t) \in \mathbb{R}^3$, with the inherent nonlinear dynamics $f : \mathbb{R} \times \mathbb{R}^3 \to \mathbb{R}^3$ described by Chua's circuit

$$f(t, x_i) = \left(\zeta\left(-x_{i1} + x_{i2} - l(x_{i1})\right), x_{i1} - x_{i2} + x_{i3}, -\chi x_{i2}\right)^T, \tag{35}$$

where $l(x_{i1}) = b x_{i1} + 0.5(a-b)(|x_{i1}+1| - |x_{i1}-1|)$. While choosing $\zeta = 10$, $\chi = 18$, $a = -4/3$, and $b = -3/4$, system (35) is chaotic with the Lipschitz constant $\eta = 4.3871$ [19] as shown in Figure 8. Assume that the state of each agent is corrupted by white noise $w_i(t) \in \mathbb{R}^3$ with the noise power $\xi = \left[0.25\ 0.25\ 0.25\right]^T$.

5.1. Case 1: strongly connected

The digraph is strongly connected as shown in Figure 5(a). From (22), multi-agent system can be translated into the edge Laplacian dynamics associated with the edge-interconnection digraph shown in Figure 5(b). The incidence matrix E and the edge adjacency matrix A_e are

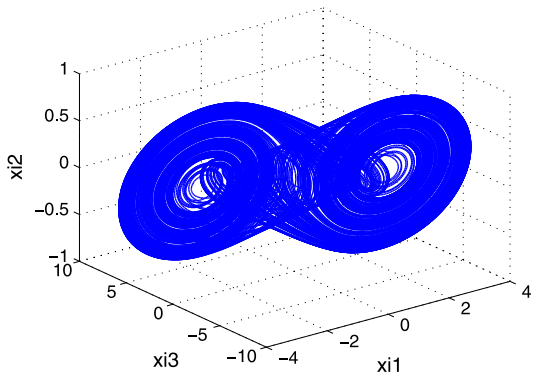

Figure 8. Chaos with two attractors.

DOI: 10.1002/rnc

$$E = \begin{pmatrix} -1 & 1 & 0 & 0 & 0 & 0 & 0 & 0 \\ 1 & 0 & -1 & 1 & -1 & 0 & 0 & 0 \\ 0 & -1 & 0 & 0 & 0 & 1 & -1 & 1 \\ 0 & 0 & 1 & -1 & 0 & 0 & 0 & 0 \\ 0 & 0 & 0 & 0 & 1 & -1 & 0 & 0 \\ 0 & 0 & 0 & 0 & 0 & 0 & 1 & -1 \end{pmatrix},$$

$$Ae = \begin{pmatrix} 0 & -1 & 0 & 1 & 0 & 0 & 0 & 0 \\ 0 & 0 & 0 & 0 & 0 & -1 & 0 & -1 \\ -1 & 0 & 0 & -1 & 0 & 0 & 0 & 0 \\ 1 & 0 & -1 & 0 & 0 & 0 & 0 & 0 \\ -1 & 0 & 0 & -1 & 0 & 0 & 0 & 0 \\ 0 & 0 & 0 & 0 & -1 & 0 & 0 & 1 \\ 0 & 0 & 0 & 0 & 0 & -1 & 0 & -1 \\ 0 & 0 & 0 & 0 & 0 & 1 & -1 & 0 \end{pmatrix}.$$

Then the edge Laplacian can be calculated though $Le = I + Ae$.

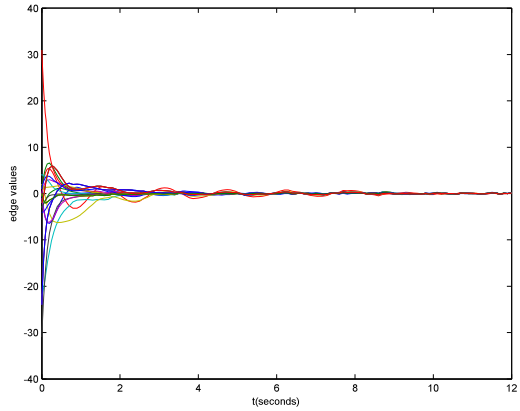

(a) The edge agreement is achieved under control law (23) and (24).

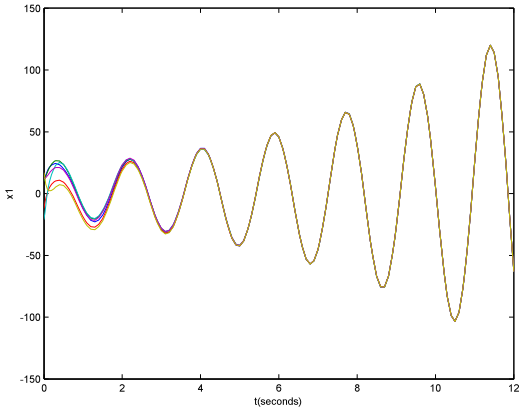

(b) The evolutions of x_{i1}.

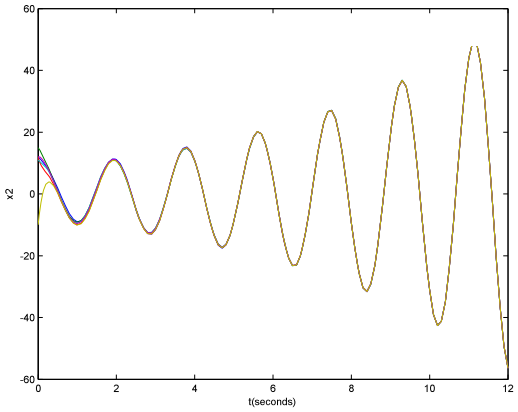

(c) The evolutions of x_{i2}.

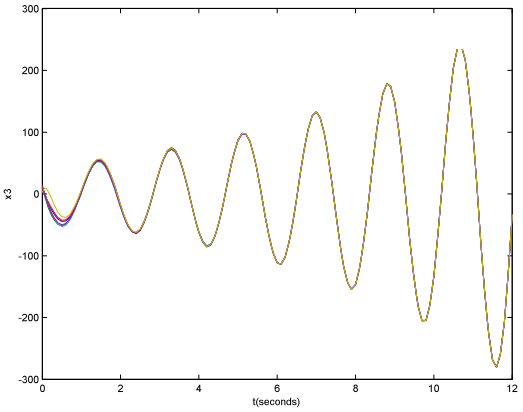

(d) The evolutions of x_{i3}.

Figure 9. The simulation results under strongly connected digraph.

DOI: 10.1002/rnc

By simply choosing $\gamma_{\tilde{x}_{e_k}}^{\tilde{x}_{e_l}} < \mathrm{Id}$ with $k, l = 1, 2, \cdots, 8, e_l \in N_{e_k}^{\otimes}$, the cyclic-small-gain theorem condition is satisfied. By taking $\gamma_{\tilde{x}_{e_k}}^{\tilde{x}_{e_l}}(s) = 0.9487s$ and $\underline{\alpha} = \overline{\alpha} = 1$, then we obtain

$$\rho_{\tilde{x}_{e_l}}^{\tilde{x}_{e_k}} = \underline{\alpha}^{-1} \circ \left(\gamma_{\tilde{x}_{e_k}}^{\tilde{x}_{e_l}}\right)^{-1} \circ \overline{\alpha}(s) = 1.0541\, s.$$

After choosing $\sigma_{e_k} = 1$, the input for the edge-interconnection system (20) is proposed as

$$\begin{aligned}
u_{e_1} &= -\frac{\tilde{x}_{e_1}}{|\tilde{x}_{e_1}|}\left(\eta|\tilde{x}_{e_1}| + 2.1082|\tilde{x}_{e_1}| + \sqrt{2}\xi\right) + 0.5\tilde{x}_{e_1},\\
u_{e_2} &= -\frac{\tilde{x}_{e_2}}{|\tilde{x}_{e_2}|}\left(\eta|\tilde{x}_{e_2}| + 2.1082|\tilde{x}_{e_2}| + \sqrt{2}\xi\right) + 0.5\tilde{x}_{e_2},\\
u_{e_3} &= -\frac{\tilde{x}_{e_3}}{|\tilde{x}_{e_3}|}\left(\eta|\tilde{x}_{e_3}| + 2.1082|\tilde{x}_{e_3}| + \sqrt{2}\xi\right) + 0.5\tilde{x}_{e_3},\\
u_{e_4} &= -\frac{\tilde{x}_{e_4}}{|\tilde{x}_{e_4}|}\left(\eta|\tilde{x}_{e_4}| + 2.1082|\tilde{x}_{e_4}| + \sqrt{2}\xi\right) + 0.5\tilde{x}_{e_4},\\
u_{e_5} &= -\frac{\tilde{x}_{e_5}}{|\tilde{x}_{e_5}|}\left(\eta|\tilde{x}_{e_5}| + 2.1082|\tilde{x}_{e_5}| + \sqrt{2}\xi\right) + 0.5\tilde{x}_{e_5},\\
u_{e_6} &= -\frac{\tilde{x}_{e_6}}{|\tilde{x}_{e_6}|}\left(\eta|\tilde{x}_{e_6}| + 2.1082|\tilde{x}_{e_6}| + \sqrt{2}\xi\right) + 0.5\tilde{x}_{e_6},\\
u_{e_7} &= -\frac{\tilde{x}_{e_7}}{|\tilde{x}_{e_7}|}\left(\eta|\tilde{x}_{e_7}| + 2.1082|\tilde{x}_{e_7}| + \sqrt{2}\xi\right) + 0.5\tilde{x}_{e_7},\\
u_{e_8} &= -\frac{\tilde{x}_{e_8}}{|\tilde{x}_{e_8}|}\left(\eta|\tilde{x}_{e_8}| + 2.1082|\tilde{x}_{e_8}| + \sqrt{2}\xi\right) + 0.5\tilde{x}_{e_8}.
\end{aligned}$$

Finally, by using (24), the consensus protocol (14) can be obtained.

The simulation results are shown in Figure 9. The edge states $\tilde{x}_{e_k}$ converge to the neighbors of the origin by applying the consensus protocol shown in Figure 9(a–d), one can see that the robust consensus is indeed achieved. Therefore, the proposed consensus protocol can effectively address the challenges resulting from the inherently nonlinear dynamics and unknown but bounded disturbances.

5.2. Case 2: quasi-strongly connected

In this case, Figure 6(a) depicts a quasi-strongly connected digraph, while Figure 6(b) illustrates its corresponding edge-interconnection digraph. The yellow nodes in Figure 6(b) correspond to $\tilde{\mathcal{G}}_{\mathcal{T}}$. According to the partition, the incidence matrix of the spanning tree $E_{\mathcal{T}}$, the incidence matrix of the co-spanning tree $E_{\mathcal{C}}$, and the edge-adjacency matrix A_e are as follows:

$$E_{\mathcal{T}} = \begin{array}{c} \begin{matrix} e_1 & e_2 & e_3 & e_4 & e_7 \end{matrix} \\ \begin{pmatrix} 1 & 1 & 1 & 0 & 0 \\ -1 & 0 & 0 & 1 & 0 \\ 0 & 0 & -1 & 0 & 1 \\ 0 & 0 & 0 & -1 & 0 \\ 0 & -1 & 0 & 0 & 0 \\ 0 & 0 & 0 & 0 & -1 \end{pmatrix} \end{array}, \quad E_{\mathcal{C}} = \begin{array}{c} \begin{matrix} e_5 & e_6 \end{matrix} \\ \begin{pmatrix} 0 & 0 \\ -1 & 0 \\ 0 & 1 \\ 0 & 0 \\ 1 & -1 \\ 0 & 0 \end{pmatrix} \end{array},$$

DOI: 10.1002/rnc

$$A_e = \begin{matrix} e_1 \\ e_2 \\ e_3 \\ e_4 \\ e_7 \\ e_5 \\ e_6 \end{matrix} \begin{pmatrix} e_1 & e_2 & e_3 & e_4 & e_7 & e_5 & e_6 \\ 0 & 1 & 1 & -1 & 0 & 0 & 0 \\ 1 & 0 & 1 & 0 & 0 & -1 & 0 \\ 1 & 1 & 0 & 0 & -1 & 0 & -1 \\ 0 & 0 & 0 & 0 & 0 & 0 & 0 \\ 0 & 0 & 0 & 0 & 0 & 0 & 1 \\ 0 & 0 & 0 & -1 & 0 & 0 & 0 \\ 0 & 0 & 0 & 0 & 1 & -1 & 0 \end{pmatrix}.$$

By simply choosing $\gamma_{\tilde{x}_{\mathcal{T}_k}}^{\tilde{x}_{\mathcal{T}_l}}(s) = 0.9487s, k, l = 1, 2, 3, 4, 7, e_l \in N_{e_k}^{\otimes}$, the cyclic-small-gain condition is satisfied. From (12), we could have

$$T = \begin{bmatrix} 1 & 0 \\ -1 & 1 \\ 0 & -1 \\ 0 & 0 \\ 0 & 0 \end{bmatrix}.$$

The smallest nonzero eigenvalue of TT^T is $\bar{\lambda}_1 = 1$; therefore, from (30), we can choose $\gamma_{\tilde{x}_{\mathcal{T}_k}}^{\tilde{x}_{\mathcal{C}}} = 0.175s$ and result to

$$\rho_{\tilde{x}_{\mathcal{T}_l}}^{\tilde{x}_{\mathcal{T}_k}} = \underline{\alpha}^{-1} \circ \left(\gamma_{\tilde{x}_{\mathcal{T}_k}}^{\tilde{x}_{\mathcal{T}_l}}\right)^{-1} \circ \overline{\alpha}(s) = 1.0541s,$$

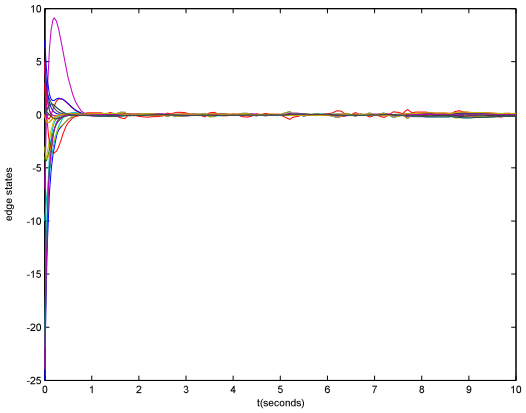

(a) The edge agreement is achieved under control law (29) and (31).

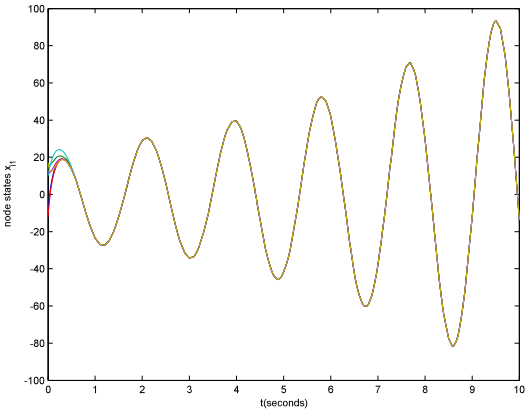

(b) The evolutions of x_{i1}.

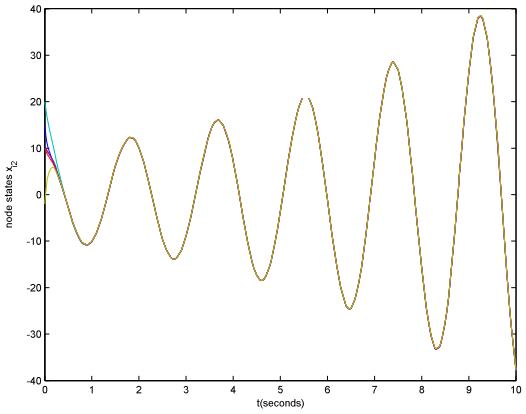

(c) The evolutions of x_{i2}.

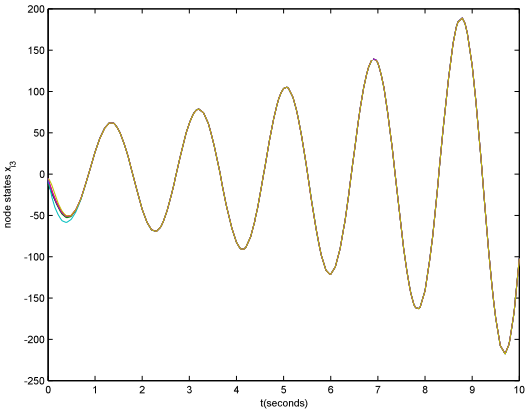

(d) The evolutions of x_{i3}.

Figure 10. The simulation results under a quasi-strongly connected digraph.

DOI: 10.1002/rnc

$$\rho_{\tilde{x}_{\mathcal{C}}}^{\tilde{x}_{\mathcal{T}_k}} = \underline{\alpha}^{-1} \circ \left(\gamma_{\tilde{x}_{\mathcal{T}_k}}^{\tilde{x}_{\mathcal{C}}}\right)^{-1} \circ \overline{\alpha}(s) = 5.7143s.$$

After taking $\sigma_{e_k} = 1$, the control input for each edge-interconnection system (20) can be determined as

$$\begin{aligned}
u_{e_1} &= -\frac{\tilde{x}_{\mathcal{T}_1}}{|\tilde{x}_{\mathcal{T}_1}|}\left(\eta\left|\tilde{x}_{\mathcal{T}_1}\right| + 3.1623\left|\tilde{x}_{\mathcal{T}_1}\right| + \sqrt{2}\xi\right) + 0.5\tilde{x}_{\mathcal{T}_1},\\
u_{e_2} &= -\frac{\tilde{x}_{\mathcal{T}_2}}{|\tilde{x}_{\mathcal{T}_2}|}\left(\eta\left|\tilde{x}_{\mathcal{T}_2}\right| + 7.8225\left|\tilde{x}_{\mathcal{T}_2}\right| + \sqrt{2}\xi\right) + 0.5\tilde{x}_{\mathcal{T}_2},\\
u_{e_3} &= -\frac{\tilde{x}_{\mathcal{T}_3}}{|\tilde{x}_{\mathcal{T}_3}|}\left(\eta\left|\tilde{x}_{\mathcal{T}_3}\right| + 8.8766\left|\tilde{x}_{\mathcal{T}_3}\right| + \sqrt{2}\xi\right) + 0.5\tilde{x}_{\mathcal{T}_3},\\
u_{e_4} &= -\frac{\tilde{x}_{\mathcal{T}_4}}{|\tilde{x}_{\mathcal{T}_4}|}\left(\eta\left|\tilde{x}_{\mathcal{T}_4}\right| + \sqrt{2}\xi\right) + 0.5\tilde{x}_{\mathcal{T}_4},\\
u_{e_7} &= -\frac{\tilde{x}_{\mathcal{T}_7}}{|\tilde{x}_{\mathcal{T}_7}|}\left(\eta\left|\tilde{x}_{\mathcal{T}_7}\right| + 5.7143\left|\tilde{x}_{\mathcal{T}_7}\right| + \sqrt{2}\xi\right) + 0.5\tilde{x}_{\mathcal{T}_7}.
\end{aligned}$$

Finally, based on (14) and (31), the implementable consensus protocol can be obtained.

Figure 10(a) shows that the edge states reach agreement by using the consensus protocol. Simultaneously, multi-agent system achieves robust consensus shown in Figure 10(b–d). Clearly, the proposed consensus protocol can effectively restrain the influences resulting from the inherently nonlinear dynamics and the unknown but bounded disturbances.

6. CONCLUSIONS

The edge Laplacian of digraph and its related concepts were originally proposed in this paper. Based on these graph-theoretic tools, we developed a new systematic framework to study multi-agent system in the context of the edge agreement. To show how the edge Laplacian sheds a new light on the leaderless consensus problem, the technical challenges caused by the unknown but bounded disturbances and the inherently nonlinear dynamics were considered, and the classical ISS nonlinear control methods together with the recently developed cyclic-small-gain theorem were successfully implemented to drive multi-agent system to reach robust consensus. Furthermore, the edge-interconnection graph, which plays an important role in the analysis and synthesis of multi-agent networks, was proposed, and its intricate relationship with the original graph was discussed. For the quasi-strongly connected case, we also pointed out a reduced-order modeling for the edge agreement in terms of the spanning tree subgraph. Based on this observation, by guaranteeing the ISS properties of each subsystem and assigning the appropriate gains for both of the interconnected subsystems to satisfy the small gain condition, the closed-loop multi-agent system could reach robust consensus. Under the edge agreement framework, we believe that nonlinear multi-agent systems with more complex factors, such as switching topologies and time delays, will be well settled.

ACKNOWLEDGEMENT

This work was supported by the National Natural Science Foundation of China under grant no. 61403406.

REFERENCES

1. Beard RW, McLain TW, Goodrich MA, Anderson EP. Coordinated target assignment and intercept for unmanned air vehicles. *IEEE Transactions on Robotics and Automation* 2002; **18**(6):911–922.
2. Lin Z, Francis B, Maggiore M. Necessary and sufficient graphical conditions for formation control of unicycles. *IEEE Transactions on Automatic Control* 2005; **50**(1):121–127.

DOI: 10.1002/rnc

3. Olfati-Saber R. Distributed Kalman filtering for sensor networks. *46th IEEE Conference on Decision and Control*, New Orleans, LA, 2007; 5492–5498. IEEE.
4. Nedic A, Ozdaglar A. Distributed subgradient methods for multi-agent optimization. *IEEE Transactions on Automatic Control* 2009; **54**(1):48–61.
5. Olfati-Saber R, Murray RM. Consensus problems in networks of agents with switching topology and time-delays. *IEEE Transactions on Automatic Control* 2004; **49**(9):1520–1533.
6. Ren W, Beard RW. Consensus seeking in multiagent systems under dynamically changing interaction topologies. *IEEE Transactions on Automatic Control* 2005; **50**(5):655–661.
7. Zelazo D, Mesbahi M. Edge agreement: graph-theoretic performance bounds and passivity analysis. *IEEE Transactions on Automatic Control* 2011; **56**(3):544–555.
8. Zelazo D, Mesbahi M. Graph-theoretic analysis and synthesis of relative sensing networks. *IEEE Transactions on Automatic Control* 2011; **56**(5):971–982.
9. Zelazo D, Schuler S, Allgöwer F. Performance and design of cycles in consensus networks. *Systems & Control Letters* 2013; **62**(1):85–96.
10. Bauso D, Giarré L, Pesenti R. Consensus for networks with unknown but bounded disturbances. *SIAM Journal on Control and Optimization* 2009; **48**(3):1756–1770.
11. Wen G, Duan Z, Li Z, Chen G. Consensus and its l_2-gain performance of multi-agent systems with intermittent information transmissions. *International Journal of Control* 2012; **85**(4):384–396.
12. Li Z, Liu X, Fu M, Xie L. Global h_∞ consensus of multi-agent systems with Lipschitz non-linear dynamics. *IET Control Theory & Applications* 2012; **6**(13):2041–2048.
13. Das A, Lewis FL. Cooperative adaptive control for synchronization of second-order systems with unknown nonlinearities. *International Journal of Robust and Nonlinear Control* 2011; **21**(13):1509–1524.
14. Zhu W, Cheng D. Leader-following consensus of second-order agents with multiple time-varying delays. *Automatica* 2010; **46**(12):1994–1999.
15. Wang X, Qin J, Li X, Zheng Z. Formation tracking for nonlinear agents with unknown second-order locally Lipschitz continuous dynamics. *31st Chinese Control Conference (CCC)*, Hefei, 2012; 6112–6117. IEEE.
16. Jie M, Wei R, Guangfu M. Containment control for multiple unknown second-order nonlinear systems under a directed graph based on neural networks. *31st Chinese Control Conference (CCC)*, IEEE, Hefei, 2012; 6450–6455.
17. Mei J, Ren W, Ma G. Distributed coordination for second-order multi-agent systems with nonlinear dynamics using only relative position measurements. *Automatica* 2013; **49**(5):1419–1427.
18. Ren W. Distributed leaderless consensus algorithms for networked Euler–Lagrange systems. *International Journal of Control* 2009; **82**(11):2137–2149.
19. Yu W, Chen G, Cao M, Kurths J. Second-order consensus for multiagent systems with directed topologies and nonlinear dynamics. *IEEE Transactions on Systems, Man, and Cybernetics, Part B: Cybernetics* 2010; **40**(3): 881–891.
20. Lin Z, Francis B, Maggiore M. State agreement for continuous-time coupled nonlinear systems. *SIAM Journal on Control and Optimization* 2007; **46**(1):288–307.
21. Shi G, Hong Y. Global target aggregation and state agreement of nonlinear multi-agent systems with switching topologies. *Automatica* 2009; **45**(5):1165–1175.
22. Sontag ED. Input to state stability: basic concepts and results. In *Nonlinear and Optimal Control Theory*. Springer: Berlin Heidelberg, 2008; 163–220.
23. Liu T, Hill DJ, Jiang Z-P. Lyapunov formulation of ISS cyclic-small-gain in continuous-time dynamical networks. *Automatica* 2011; **47**(9):2088–2093.
24. Wang X, Qin J, Yu C. Iss method for coordination control of nonlinear dynamical agents under directed topology. *IEEE Transactions on Cybernetics* 2014; **44**(10):1832–1845.
25. Liu T, Jiang Z-P. Distributed formation control of nonholonomic mobile robots without global position measurements. *Automatica* 2013; **49**(2):592–600.
26. Liu T, Jiang Z-P. Distributed output-feedback control of nonlinear multi-agent systems. *IEEE Transactions on Automatic Control* 2013; **58**(11):2912–2917.
27. Zeng Z, Wang X, Zheng Z. Nonlinear consensus under directed graph via the edge Laplacian. *The 26th Chinese Control and Decision Conference (2014 CCDC)*, IEEE, Changsha, 2014; 881–886.
28. Godsil CD, Royle G, Godsil CD. *Algebraic Graph Theory*, Vol. 207. Springer: New York, 2001.
29. Thulasiraman K, Swamy MNS. *Graphs: Theory and Algorithms*. John Wiley & Sons: Hoboken, New Jersey, 2011.
30. Isidori A. *Nonlinear Control Systems II*, Vol. 2. Springer: Berlin Heidelberg, 1999.
31. Mesbahi M, Egerstedt M. *Graph Theoretic Methods in Multiagent Networks*. Princeton University Press: Princeton, New Jersey, 2010.
32. Meyer CD. *Matrix Analysis and Applied Linear Algebra*, Vol. 2. SIAM: Philadelphia, PA, 2000.
33. Zelazo D, Rahmani A, Mesbahi M. Agreement via the edge Laplacian. *46th IEEE Conference on Decision and Control*, New Orleans, LA, 2007; 2309–2314.
34. Ben-Israel A, Greville TNE. *Generalized Inverses: Theory and Applications*, Vol. 15. Springer Science & Business Media: Berlin Heidelberg, 2003.
35. Tanner HG, Pappas GJ, Kumar V. Leader-to-formation stability. *IEEE Transactions on Robotics and Automation* 2004; **20**(3):443–455.
36. Wang X, Liu T, Qin J. Second-order consensus with unknown dynamics via cyclic-small-gain method. *IET Control Theory & Applications* 2012; **6**(18):2748–2756.

DOI: 10.1002/rnc